NBSIR 85-3289

Wide Plate Crack Arrest Tests: Instrumentation for Dynamic Strain Measurements

G. A. Danko
S. R. Low III
R. deWit
R. J. Fields

U.S. DEPARTMENT OF COMMERCE
National Bureau of Standards
Center for Materials Science
Gaithersburg, MD 20899

December 1985

Sponsored by
Oak Ridge National Laboratory
Oak Ridge, TN 37831

NBSIR 85-3289

WIDE PLATE CRACK ARREST TESTS: INSTRUMENTATION FOR DYNAMIC STRAIN MEASUREMENTS

G. A. Danko
S. R. Low III
R. deWit
R. J. Fields

U.S. DEPARTMENT OF COMMERCE
National Bureau of Standards
Center for Materials Science
Gaithersburg, MD 20899

December 1985

Sponsored by
Oak Ridge National Laboratory
Oak Ridge, TN 37831

U.S. DEPARTMENT OF COMMERCE, Malcolm Baldrige, *Secretary*
NATIONAL BUREAU OF STANDARDS, Ernest Ambler, *Director*

WIDE PLATE CRACK ARREST TESTS: INSTRUMENTATION FOR DYNAMIC STRAIN MEASUREMENTS

G.A. Danko, S.R. Low III, R. deWit and R.J. Fields
Institute for Materials Science and Engineering
National Bureau of Standards
Gaithersburg, Maryland 20899

Abstract:
A series of crack arrest tests on large (10 x 1 x 0.1 m) steel plates is described. Special emphasis is placed on the description of the temperature gradient, relevant instrumentation, strain gaging, and data collection systems. Circuit diagrams are given for the bridges and multichannel dynamic amplifiers that were constructed specifically for this type of testing.

Key Words: Amplifier; arrest; bridges; cracks; dynamic; fracture; instrumentation; tape recorder.

Introduction:

As part of the Heavy Section Steel Technology Program sponsored by the Nuclear Regulatory Commission and managed by Oak Ridge National Laboratory, the National Bureau of Standards has performed two large crack arrest tests[1]. The most recent of these, WP-1.2, will be discussed here. The specimen is shown schematically in Figure 1a. The actual specimen mounted in the NBS 25 MN testing machine is shown in Figure 1b. Welded into the center of the specimen is a specially prepared plate of well characterized A533B steel containing a notch and sharp crack and which is face-grooved to provide some means of directing the crack. These specially prepared plates were supplied and fabricated by Oak Ridge National Laboratory[2].

These specimens are first heated and cooled on the edges to establish a nearly linear temperature gradient across the 1 meter width. They are then loaded in uniaxial tension until crack propagation initiates[3,4,5]. The specimens are instrumented with about 20 strain gages and 30 thermocouples each. In addition, crack mouth opening gages and timing stripes are used. The outputs of the various instruments are followed throughout the development of the temperature gradient, the loading up, and the fracture event. This paper describes the methods used to develop the linear thermal gradient across the specimen, and details the instrumentation that is used to monitor temperature and the response of the various strain gages.

Temperature Gradient:

In the region of the face grooves, which becomes the fracture plane, the thermal gradient must be nearly linear having a range of -95°C (-139°F) at the cooled, notched edge to 205°C (401°F) at the opposite heated edge. To produce a linear temperature gradient, the specimen is heated and cooled only on the 10 cm (4 in) thick edge surfaces of the plate. Appropriate thermal insulation is attached to the plate faces, which are not directly heated or cooled. Specimen temperature is monitored by a data acquisition system using thermocouples at various locations both near the fracture area and at far-field locations on the pull plates. These techniques are detailed in the following.

Specimen Heating and Cooling:

Heating of the specimen is accomplished with eight individual electric resistance strip-heaters. Each heater is 3.8 cm (1.5 in) wide with a heat element length of 61

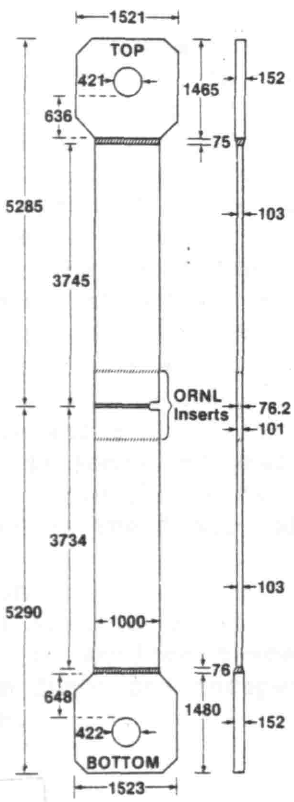

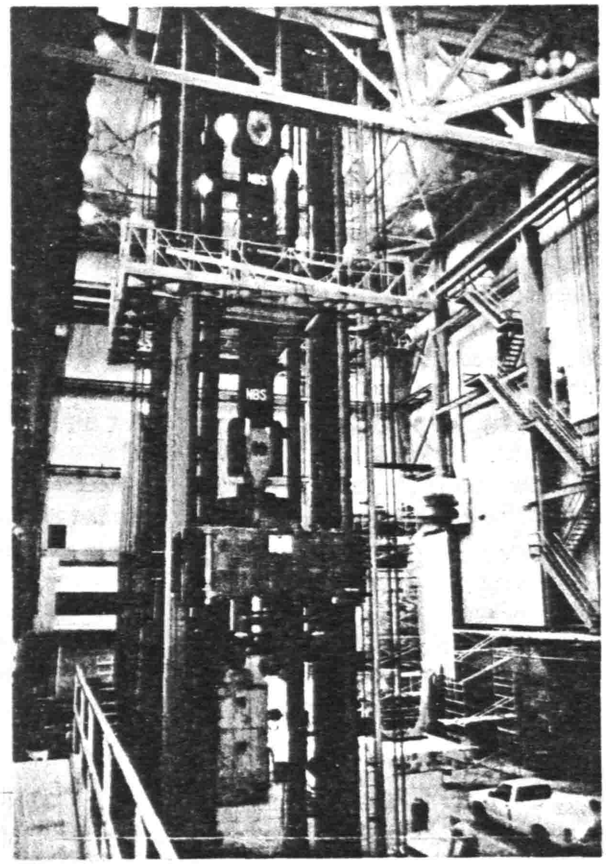

Figure 1. a) Schematic drawing of specimen. All dimensions are in millimeters. b) Specimen mounted in testing machine. Note truck in lower right corner for approximate scale.

cm (24 in) rated at 1.9W/cm^2 (12.0 W/in^2). The heaters are attached to the edge of the plate in pairs and are backed with a 1.3 cm (0.5 in) thick sheet of Marinite I* insulating board to hold the heater against the plate surface as well as for thermal insulation.

Heating level is controlled by two means. Firstly, the power level or heat output of each heater can be varied through a separate variac transformer. Secondly, two zones of heating are controlled by separate on/off type temperature controllers monitoring thermocouple sensors at the heated edge of the specimen. The primary heating zone is formed by the 2 pairs of heaters attached to the specimen edge on either side of the fracture plane. The second zone consists of the two areas on either side of the first zone and are heated by the outward 2 pairs of heaters. Temperature levels in the two zones are independently controlled to better achieve and maintain a linear gradient across the specimen.

The cold edge of the specimen is cooled by spraying liquid nitrogen (LN2) onto the noteched edge of the specimen. A 2.6 m (8.5 ft) long insulated chamber is affixed to the specimen edge, equally spanning both sides of the notch. The LN2 is pumped into the chamber and sprayed directly onto the specimen surface with a copper tube manifold constructed of sprayers at 18 cm (7 in) increments. The cooling level is controlled by two methods. Initially, when establishing a linear gradient, the temperature is controlled by adjusting the LN2 flow rate by manually setting a hand valve. When the desired temperature is achieved, that level is maintained by controlling the LN2 flow with an on/off type temperature controller that monitors a thermocuple at the cold edge of the specimen. The temperature controller powers an electric solenoid gas-valve that can stop or allow the flow of LN2 into the cold chamber. Once the desired thermal gradient is achieved, it can be maintained solely by the three temperature controllers for the heaters and cold chamber.

Two types of thermal insulation are used to insulate the front and back faces of the specimen. On the hot side of the plate, 5 cm (2 in) thick mineral wool bats are used having a width of 61 cm (24 in). They are positioned on the specimen face at the vertical center line of the specimen extending beyond the heated edge and the strip heaters. The cold side is similarily insulated with 61 cm (24 in) wide and 5 cm (2 in) thick styrofoam sheets, by butting against the mineral wool at the specimen center and extending beyond the cooled edge or to the cold chamber. The cold chamber is also insulated with 2.5 cm (1.0 in) thick styrofoam. In both cases the specimen insulation is held snugly against the plate surface covering an area 3 m (10 ft) above and 3 m (10 ft) below the fracture plane on both the front and back surfaces. Additional mineral wool and styrofoam insulation is placed on the specimen edges above and below the heaters and cold chamber covering the same length on the specimen as the front and back face insulation.

Instrumentation:

The overall system is shown schematically in Figure 2. It consists of two sub-systems: one to monitor temperature and one to monitor strain and other gages. Each subsystem functions independently and is monitored or controlled by a separate micro-computer.

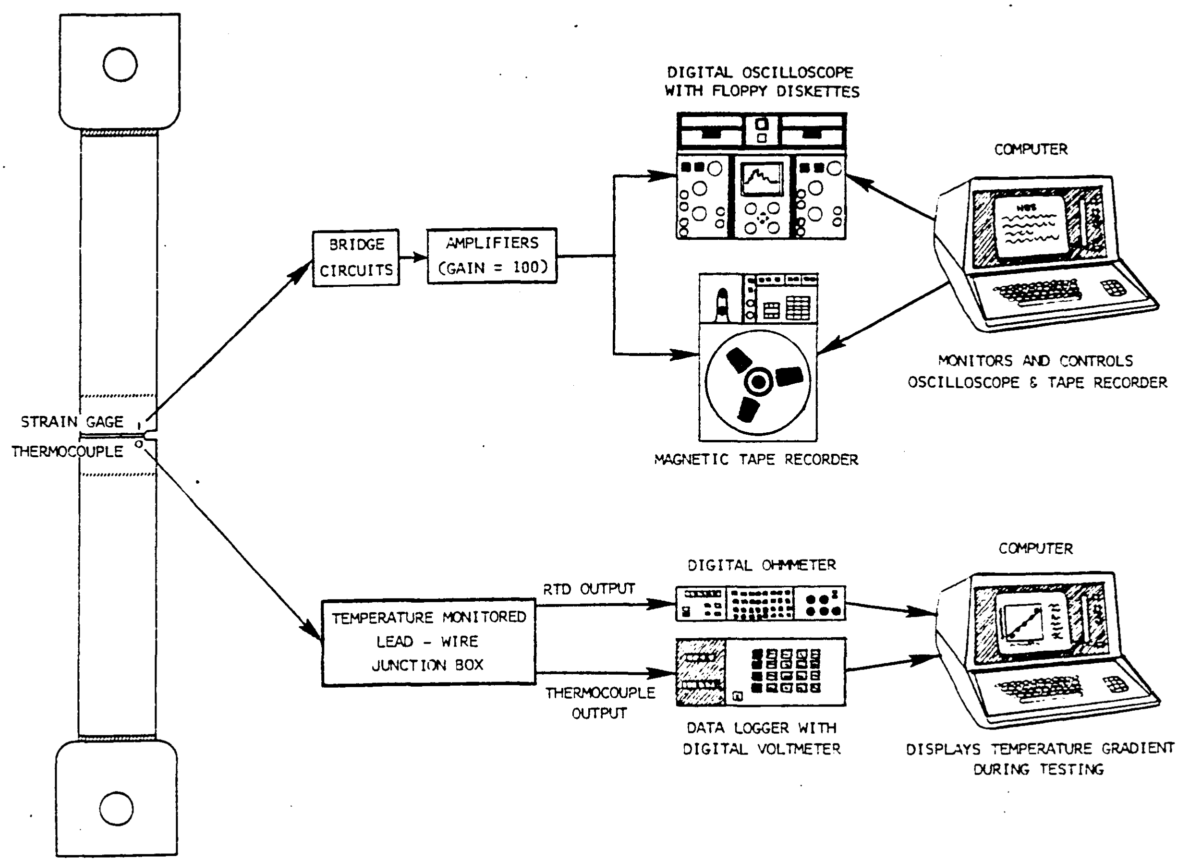

Figure 2. Data acquisition system.

The temperatures at various locations on the specimen are monitored by thermocouple sensors. The near-field thermocouples are positioned as shown in figure 3. Each thermocouple is attached by inserting it into a 0.16 cm (0.06 in) diameter hole that is drilled to a depth of about 0.30 cm (0.12 in) into the surface of the specimen. The hole and thermocouple are then covered with a protective silicone coating. The system to monitor the thermocouples is shown schematically in the lower portion of Figure 2. The thermocouple lead-wires are connected to pairs of copper wires in a thermally insulated junction box. The copper wires are connected to a data logger which, at designated time intervals, sequentially measures the millivoltage produced by each thermocouple. The temperature within the junction box is measured with a Resistance Temperature Detector (RTD) that is monitored by a digital ohmmeter. A computer, interfaced with both the data logger and ohmmeter, is then used to calculate the measured temperature data, display the data, and store the data onto magnetic tape.

During the heating and cooling processes, the 11 thermocouples adjacent to the face-groove (numbered 0 thru 10 in Figure 3) are monitored to characterize the temperature gradient at the fracture plane. The actual temperature values are displayed graphically with the desired linear gradient indicated as a line on the graph as shown in Figure 4. The additional thermocouple data also can be displayed in real time, but is primarily stored for post-test analysis.

As seen in the upper portion of figure 2, the strain gages are connected directly to bridges, the imbalance of which is first amplified by wide band differential amplifiers and then recorded either on a transient digitial oscilloscope or on a wide band, frequency modulated tape recorder. Both of these last two recording devices are under the control of a dedicated micro-computer. Each component of this system is described in detail in the following.

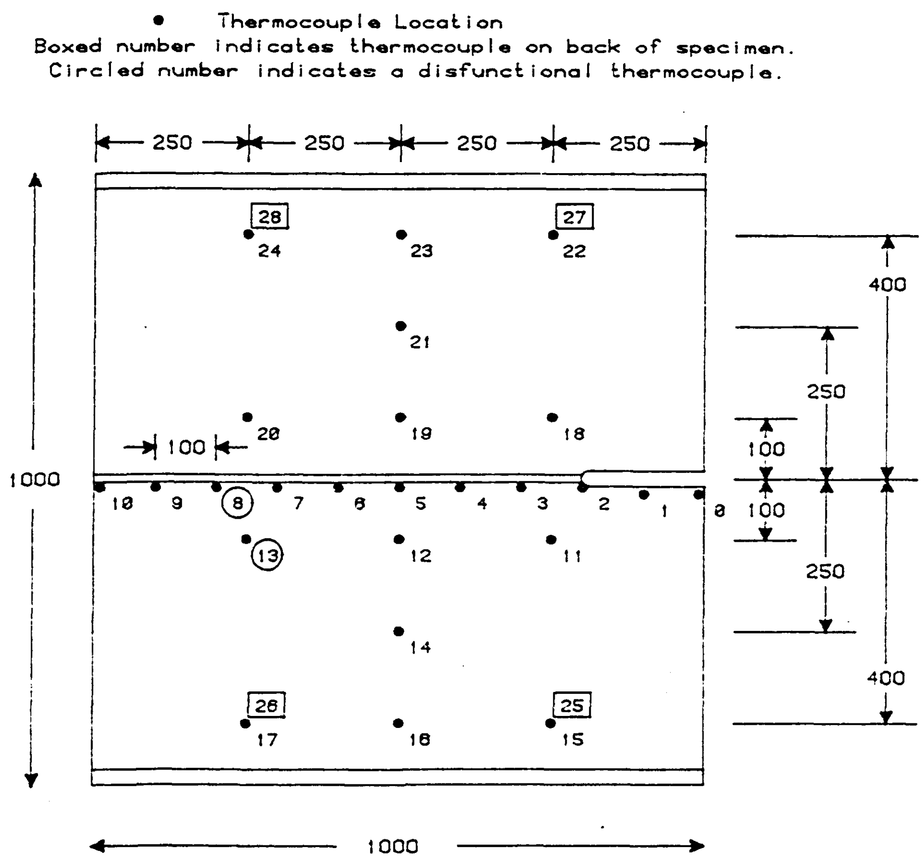

Figure 3. Positions of thermocouples on wide plate test specimen. All dimensions are in millimeters.

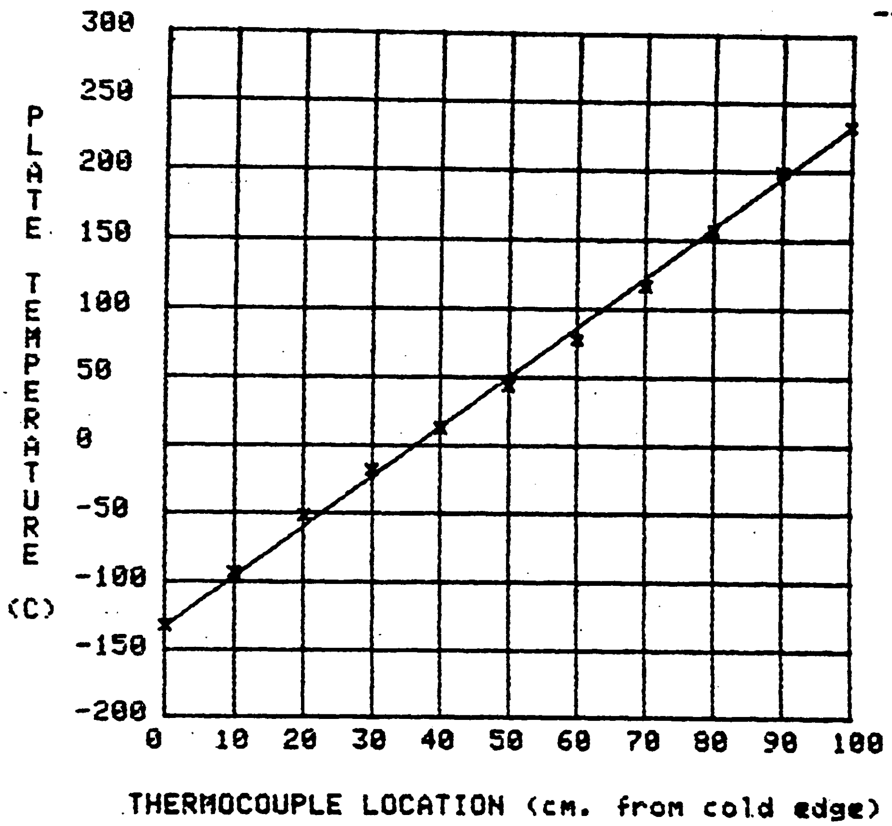

cm	TEMPERATURE (C) actual	TEMPERATURE (C) desired
0	-132	-133
10	-94	-97
20	-52	-60
30	-18	-24
40	12	13
50	44	50
60	77	86
70	117	123
80	158	159
90	200	196
100	233	233

Figure 4. Real-time display of temperature gradient.

Strain Gages:

The positions of the near-field strain gages on the plate are shown in Figure 5. For brevity only the crack-line gages will be covered in detail here since the procedures discussed could apply to all strain gaging on the specimen. The crack line gages were 90° stacked, 350 ohm, Karma* alloy gages on polyimide backing. One set consists of two pairs of gages (a longitudinal one and a transverse one) mounted across the crack plane from each other. These were mounted on the specimen using a standard epoxy, cured for 2 hours at 149°C (300°F) and post-cured for 4 hours at 232°C (450°F). The longitudinal gages were connected in series to one side of a bridge and the transverse gages were connected in series to the other side. This approach cancels out temperature effects in the gages. This is important since the plate is subjected to an extreme temperature variation. However, this approach makes the bridge output proportional to the difference in the longitudinal and transverse strains. While this effect does not detract from the value of the data collected, it must be borne in mind during any analysis of the results.

Bridges:

The bridge circuit used for these tests is shown schematiclly in Figure 6. This type of circuit is a routine one for strain gage bridges[6]. The actual bridge is unique in that every effort was made to reduce reactance to a low level so that the bridge could monitor the high strain rate changes during the fracture event with a minimum of distortion. To this end, all wire wound resistors (whether variable or fixed) were avoided to minimize inductance. Instead, cermet potentiometers and tin oxide

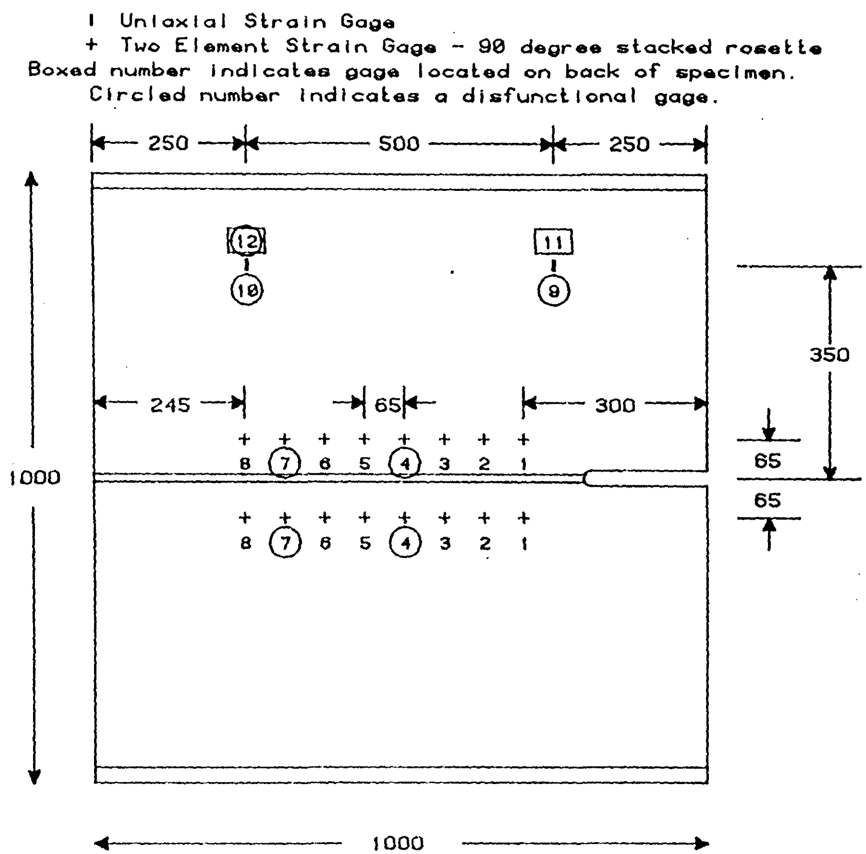

Figure 5. Positions of strain gages on wide plate test specimen. All dimensions are in millimeters.

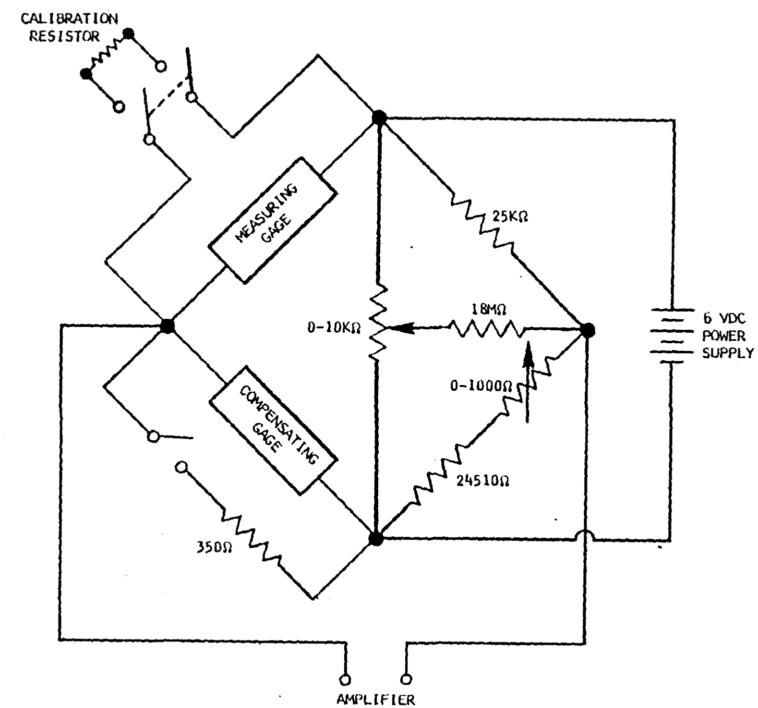

Figure 6. Bridge circuit diagram for strain gages.

resistors were used for the resistive bridge components. Connections were made with twisted pairs instead of coaxial cables, where possible, to reduce capacitance and to increase common-mode rejection. All bridges for the crack-line gages were constructed in an identical fashion and mounted in a shielded metal box whose case was connected to earth. A convenient feature of these bridges was a connection for a calibration resistor. The calibration resistor could be switched in and out of one leg of each bridge by means of a switch. For these tests, it was found that energizing the bridges using 6 volt batteries produced satisfactory results. In the future, higher voltages will be considered to improve the signal-to-noise ratio.

Amplifiers:

A printed circuit board containing eight wide-band differential amplifiers was developed expressly for this test series. The circuit diagrams for each channel is shown in Figure 7. The heart of the circuit is the Analog Devices* AD521KD instrumentation amplifier. Gain is set by the ratio of two external resistances R_S and R_G. The gain equation is fairly precise (±0.3% absolute); gain setting is accomplished by adjusting the gain trim potentiometer so that R_S equals 100 times R_G to within 10 ppm. This adjustment is performed with the AD521 out of circuit.

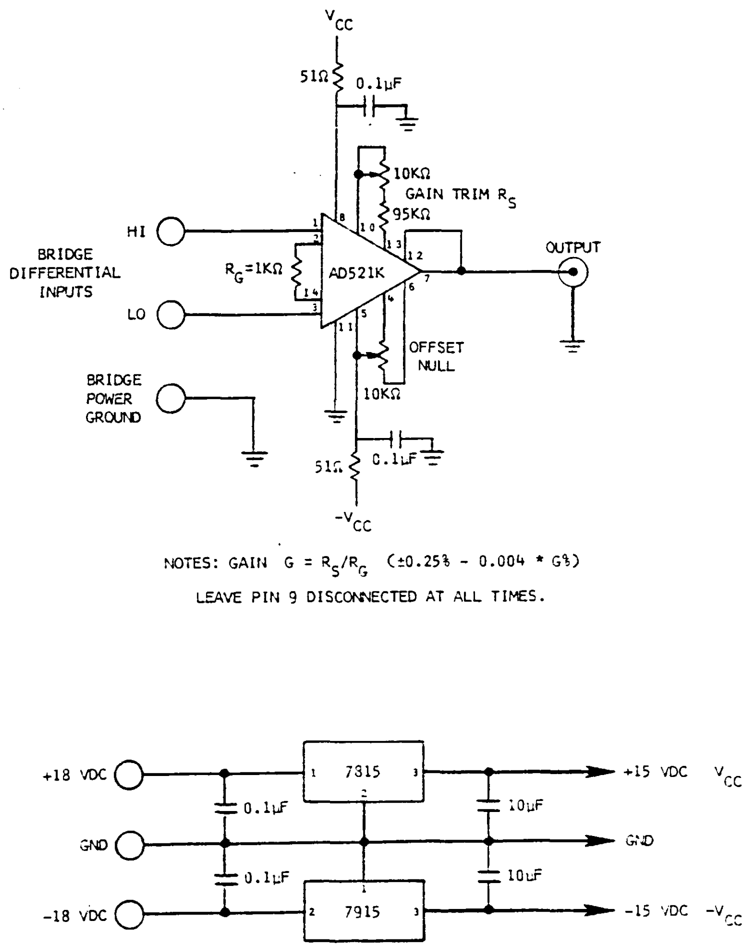

Figure 7. Circuit diagram for one amplifier channel.

The circuit board itself is of the double-sided glass-epoxy type. The component side of the board is used as a ground plane to help reduce spurious interference. The AD521 is soldered directly to the board to keep the device close to the ground plane. Input and output lines are twisted pairs to minimize common-mode effects.

The ground potential of the amplifier is connected to bridge power ground. This establishes a zero volt reference for the amplifier, i.e., they are DC coupled to the bridges. An accurate reading of the differential input voltage is thus attained, while the high input impedance inherent in instrumentation amplifier design minimizes loading of the strain gage bridge.

The calculated frequency response is typically 200kHz (±3dB), with a common mode rejection ratio of 114 dB and 123 μV RMS noise. Since the typical strain pulse is on the order of 100 kHz and 7 mv, contributions to the signal by the amplifiers were dismissed as negligible.

Recording of Strain Gage Response:

As shown in Figure 2, the amplified bridge outputs are sent to both transient digital oscilloscopes and to a wide band frequency modulated, magnetic tape recorder. The oscilloscopes were set to trigger off a strain gage output and their windows were wide enough to record only the fracture event. The tape recorder did not require triggering and it recorded the entire loading sequence for nearly 30 minutes up to and including the fracture event. The tape recorder was run at 60 inches per second for this test. At this speed, the recorder provides a distortion-free record from DC to 250 KHz.

Both the oscilloscopes and the recorder were under direct control of a micro-computer by means of a GPIB (IEEE-488 1978) connector. This remote control was required because both recording instruments, as well as all amplifiers and bridges, were located close to the actual fracture location. This was on a platform attached to the testing machine and 50 feet above floor level. The decision to keep all equipment near the test was made on the basis of reducing noise and to eliminate difficulties associated with sending many transient signals down long cables. The controlling computer could remotely set and reset the trigger and window settings on the oscilloscopes. It could also start, stop, rewind, and set recording speeds on the tape recorder.

Results and Discussion:

The usefulness of the above systems can only be judged by how well they performed during the experiment. Consider first the strain gages during the development of the temperature gradient. By cooling one edge of the plate to -95°C and heating the other to 205°C, an approximately linear temperature gradient of 3°C per centimeter was obtained. A linear temperature gradient results in a stress-free strain. Since the thermal expansion coefficient of the gages was matched to that of steel, the gages should register zero strain in such a linear gradient. However, during the development of the gradient, there is a period of extreme non-linearity in the temperature distribution. During this period, the gages should register some strain. Therefore, the strain gages should start at zero, go through a peak, and return to zero as the gradient becomes linear. Figure 8 shows the response of gage #3 (se figure 2 for its position on the plate) during the temperature gradient development. The time axis in Figure 8 extends over about 10 hours and indicates the relative stability of the various bridges, amplifiers, and power supplies. As discussed above, the strain starts near zero, goes through a peak, and returns to near zero. This is just as expected.

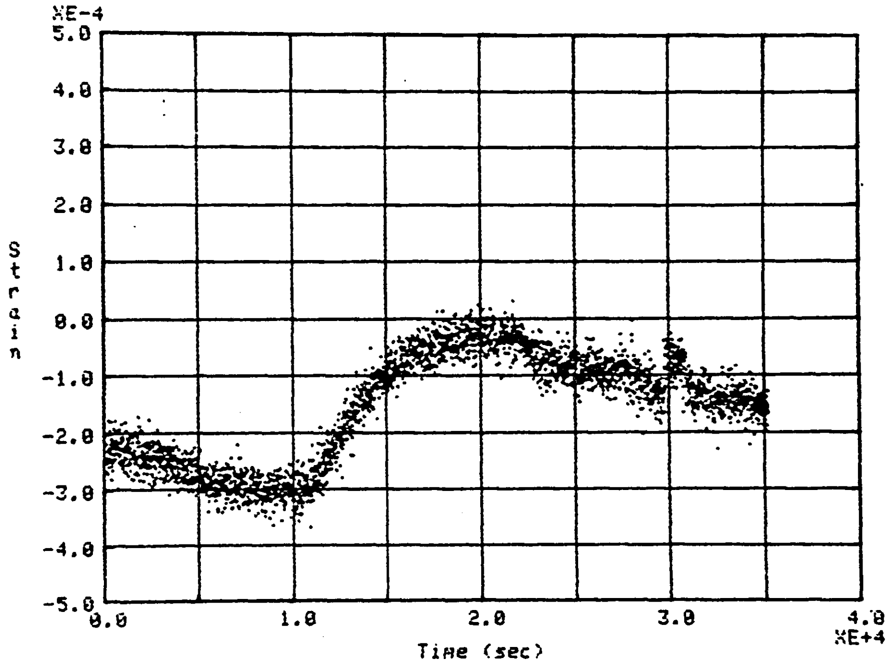

Figure 8. Strain recorded by strain gage #3 during development of temperature gradient.

Now consider the loading up period just before fracture. Since fracture occurred well below the plastic yielding load, most of the gages should simply be straight lines. Since the crack-line gages are located near a notch, their slopes will not be Young's modulus. In Figure 9, the responses of strain gages 1, 2, and 3 are shown during the loading up period. Note that the slopes are basically linear although #1 (closest to the notch) shows a slight non-linear tendency. Also, the slopes become less steep the farther the gages are from the notch. This is to be expected and data like these are useful in determining the singular and non-linear components of the stress field near a crack.

Finally, the real test of the system comes during the fracture event. This total event is over in about 20 ms. The propagation and arrest of the cleavage crack occurs in 1 to 2 ms and enough resolution is required to observe the fine details of this part of the event. When the crack starts moving, a sudden increase in strain should be registered by each gage. The strain should increase rapidly as the crack approaches a gage and peak just before the crack goes under the gage, then fall rapidly to zero as the crack extends past the gage. The responses of gages #1, 2, and 3 during the fracture event are shown in Figure 10. These data exhibit the features discussed above and can be used to locate the approximate position of the crack tip during this rapid event. In this way, the average crack velocity between various positions can be calculated and is listed in Table 1. In the future, it is hoped to use the continuous strain output, rather than just the peak, to locate the tip with much greater precision. In addition, these strain records provide crack velocity as a function of stress intensity factor for analysis of dynamic fracture situations.

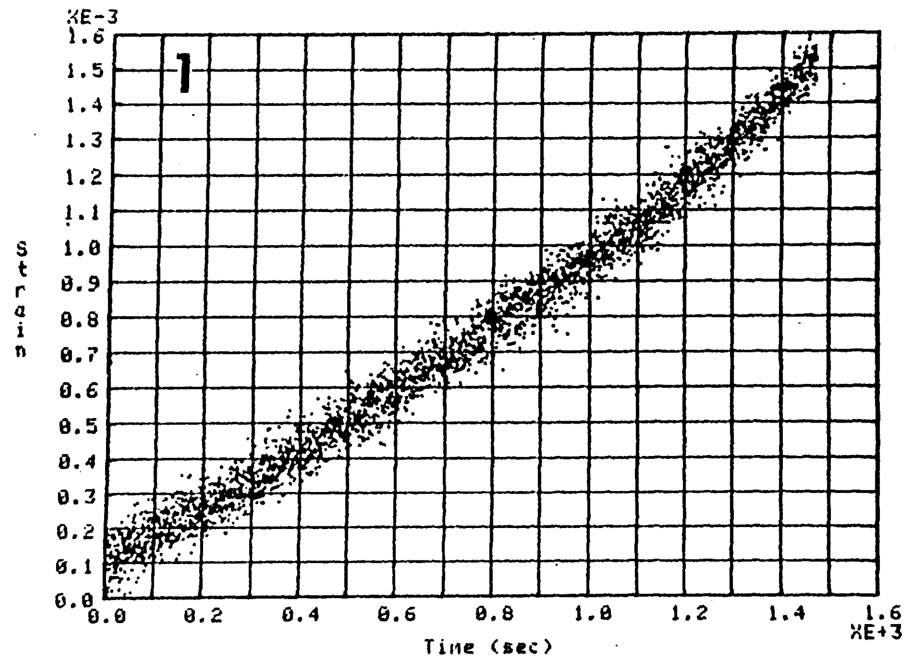

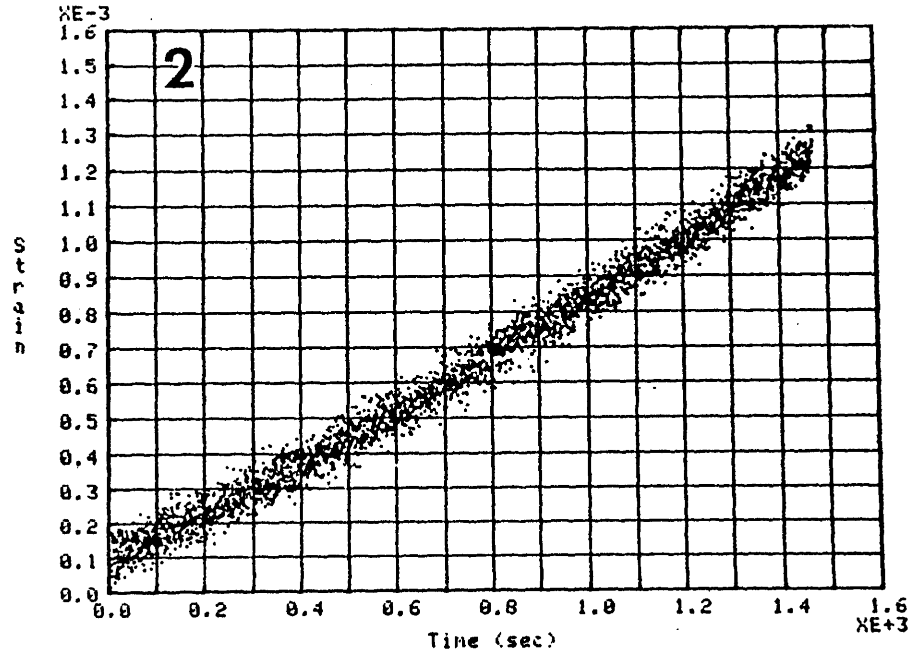

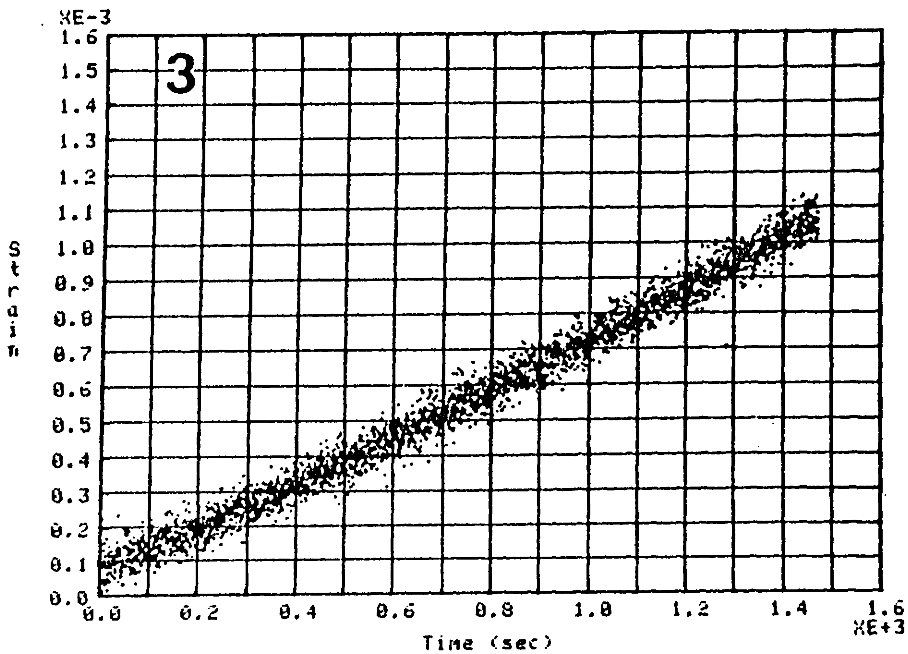

Figure 9. Responses of strain gages #1, 2, and 3 during the loading up to fracture.

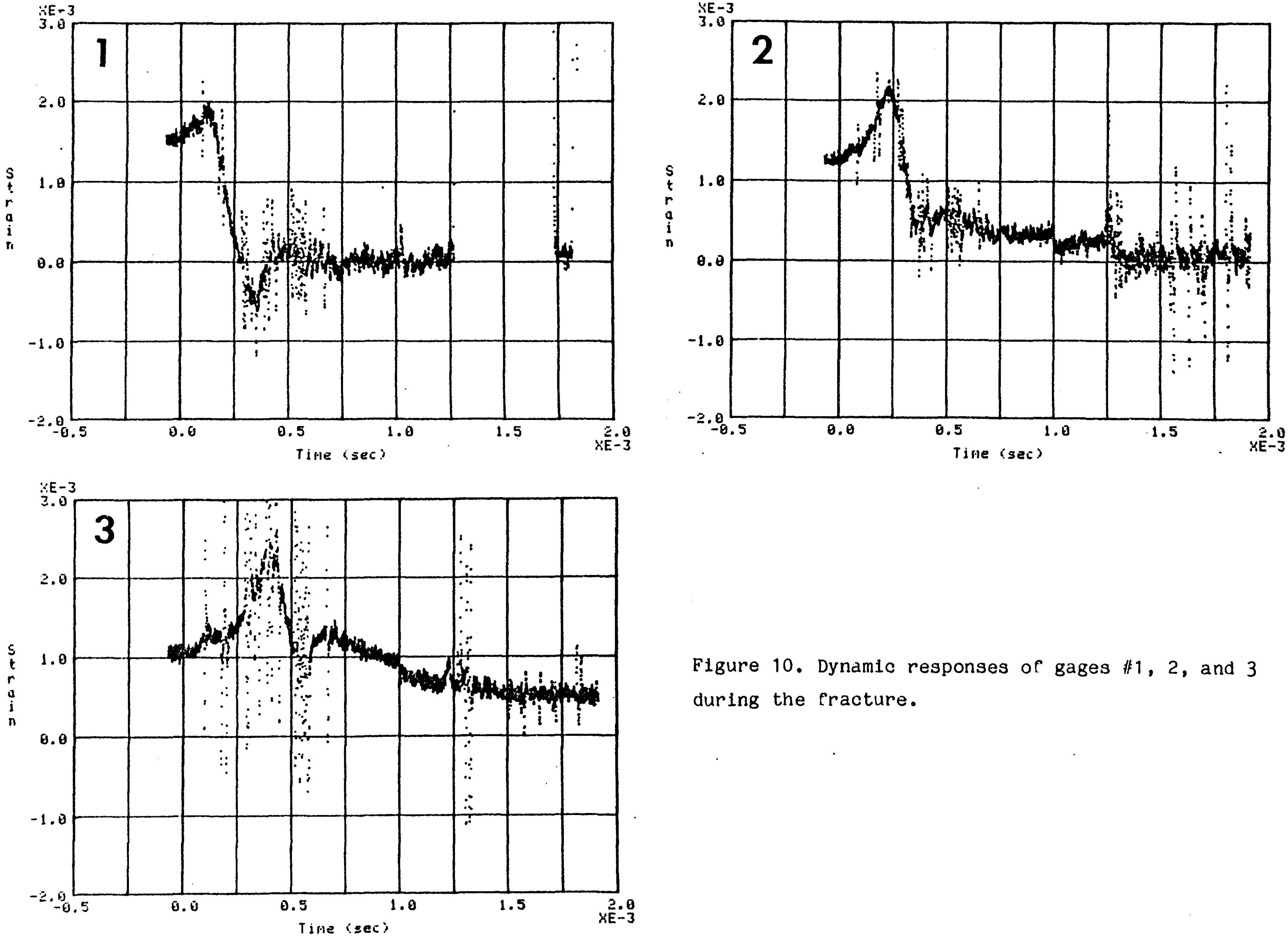

Figure 10. Dynamic responses of gages #1, 2, and 3 during the fracture.

TABLE 1.

Crack Position (mm)	Time (ms)	Velocity (m/s)
199	0	
300	0.125	808
365	0.234	599
430	0.396	401
555	0.966	219
555	1.866	0
645	2.806	96
645	3.586	0
1000	15.226	30

Strain gage #8 (see Figure 11) shows rather different characteristics from the previous strain gage outputs. The strain starts to increase, but then levels off for almost a millisecond. After this pause, the strain once again increases only to level off a second time. After this pause, the strain increases until the gage is plastically pinned and no further change can be registered. Examining the fracture surface in Figure 12, one notes the presence of two arrests indicated by arrows. The pauses in the strain gage #8 record are due to the sudden stopping or pausing of the crack at these points. Thus, the strain gages not only provide information about crack position and stress field, but also provide unambiguous evidence of crack arrest during a rapid fracture event.

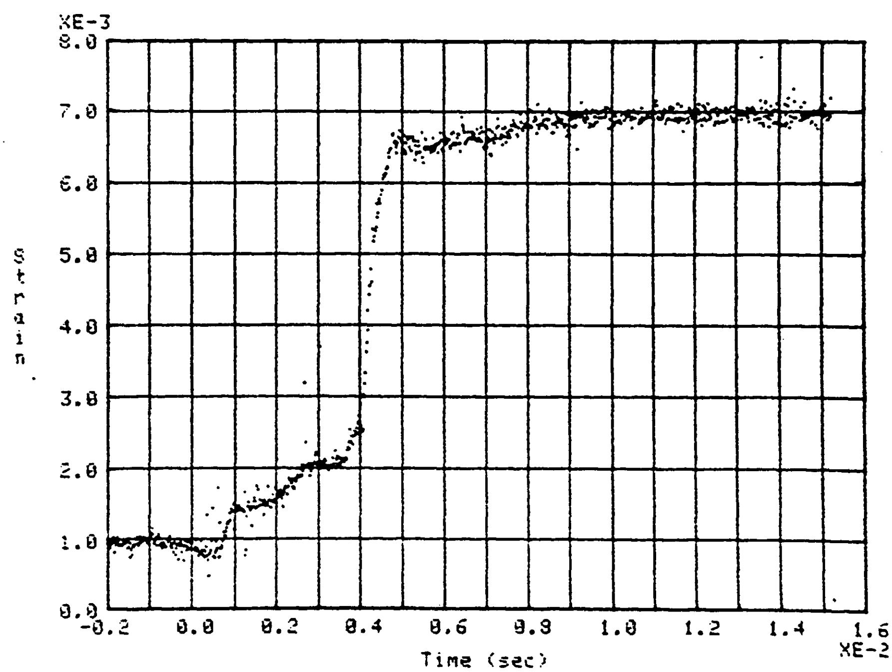

Figure 11. Dynamic response of gage #8 during the fracture event.

Finally, it is instructive to compare the results recorded on the oscilloscopes with those recorded on the tape recorder. Figure 13 compares the output of strain gage #2 recorded on the tape and on the oscilloscope. The strain levels are in perfect agreement. This implies that both recording methods are accurate. The oscilloscope record does not have the time resolution that can be obtained from the magnetic tape. Of course, the window on the oscilloscope could have been made smaller, but this risks missing the critical events if the triggering does not occur at the correct time. The taped record, while having better time resolution, is noisier, 32dB typical at 2 MHz. The noise, however, can be reduced by appropriate filtering of the tape recorder output during playback (see Figure 14). Therefore, the tape recorder provides as good or better a record of the fracture event as the transient oscilloscope and it does not risk the loss of data due to the misfiring of a triggering system. In addition, the tape recorder is less costly per data channel than the oscilloscope.

Conclusions:

A method has been developed for producing an approximately linear thermal gradient across the 1.0 m (3.3 ft) width of a 10 cm (4 in) thick steel specimen in the region of expected fracture. The temperature gradients produced in the specimens for the two completed tests have been satisfactorily linear to allow interpolation of temperatures at any location along the fracture path.

A system for acquiring temperature data from over 30 thermocouples has been designed, which can sample each sensor and display the data in real time. The computer display of the actual versus the desired temperture gradient simplifies the task of monitoring and adjusting the heating and cooling systems to achieve and maintain a linear gradient. The magnetic tape storage of the data allows the recalling of the specimens temperature profile throughout the stages of testing.

A data acquisition system for crack arrest testing has been designed. It consists of low reactance bridges, wide-band amplifiers, and a multichannel wide-band, frequency modulated tape recorder controlled by a micro-computer. The results obtained using this system indicate that it correctly acquires the data during rapid events. Furthermore, the system described here provides a high probability that no data will be lost during dynamic events provided the gages themselves remain operational.

Using this system the position of a crack moving through a one meter wide plate has been monitored with microsecond resolution. From this data, crack velocities have been determined and unambiguous evidence of a crack arrest is presented. Thus, the value to dynamic fracture studies of using strain gages in conjunction with the present instrumentation is demonstrated.

Acknowledgement:

The authors would like to express their gratitude to Milton Vagins of the Nuclear Regulatory Commission and Claud E. Pugh of Oak Ridge National Laboratory for their encouragement and support during the performance of the research described here. In addition, the authors thank Joseph Sanford of the University of Maryland for numerous useful suggestions concerning strain gaging, many of which are employed in the present testing program.

---

*Trade names and companies are identified in order to adequately specify the experimental procedure. In no case does such identification imply recommendation or endorsement by the National Bureau of Standards, nor does it imply that the products are necessarily the best available for the purpose.

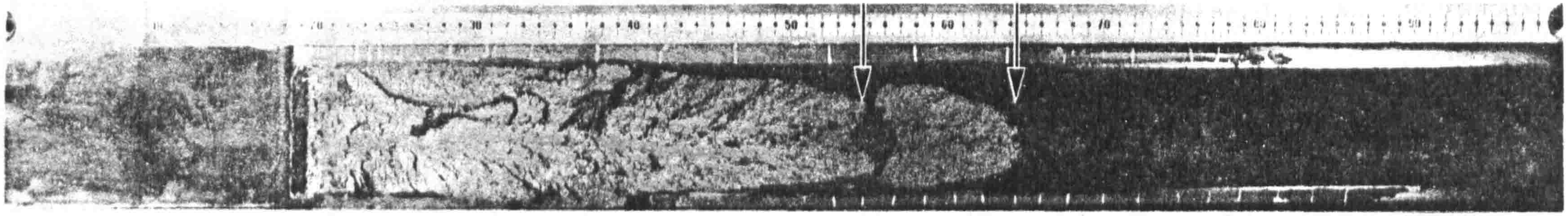

Figure 12. Fracture surface of the second wide plate test (WP-1.2). Note arrests which are indicated by arrows.

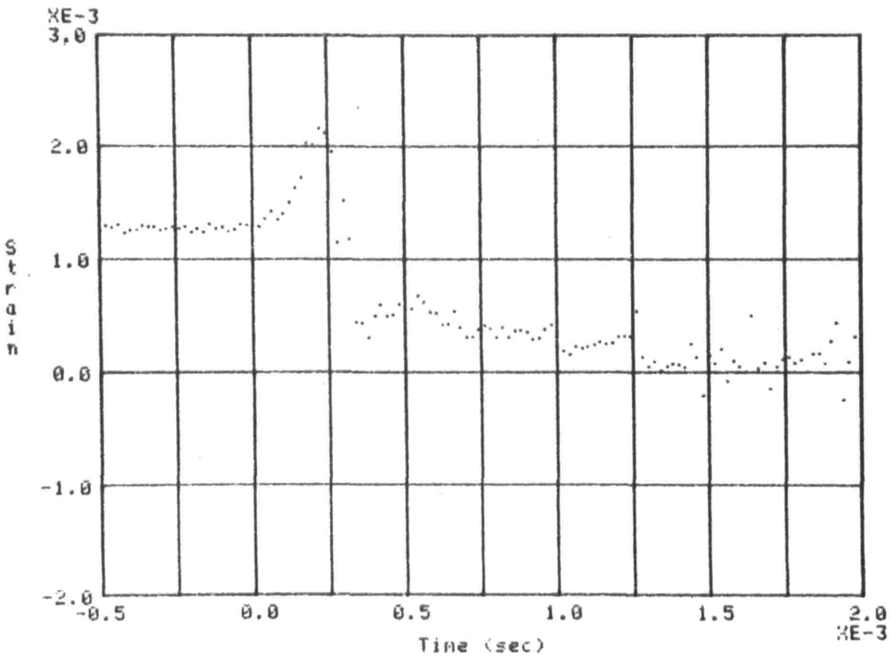

Figure 13. Data acquired by transient oscilloscope for strain gage 2. Compare with unfiltered, recorded signal in Figure 10 or with digitially filtered, recorded signal in Figure 14.

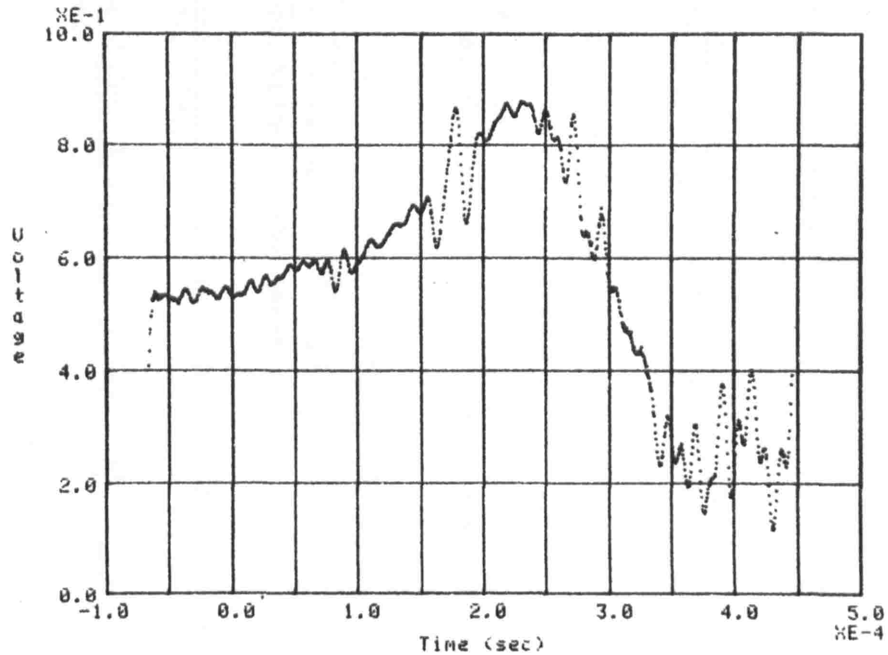

Figure 14. Digitally filtered signal from magnetic tape recorder.

References:

1.) Heavy-Section Steel Technology Program, Five-Year Plan, FY1984-1988, Oak Ridge National Laboratory, NUREG/CR-4275 and ORNL/TM-9654, July 1985.

2.) Heavy-Section Steel Technology Program, Semiannual Progress Report for October 1984-March 1985, Oak Ridge National Laboratory, NUREG/CR-4219 Volume 1 and ORNL/TM-9593/V1, June 1985.

3.) T.S. Robertson, "The Robertson Crack Arrest Test," Brithish Welding Journal, 15, pp 387-394, (1968).

4.) J. Eftis and J.M.Kraft, "A Comparison of the Initiation with the Rapid Propagation of a Crack in Mild Steel Plate," Journal of Basic Engineering (Trans ASME) 87, pp 257-263, (1965).

5.) T. Kanizarva, S. achiaa, and H. Yajima, "Recent Studies on Brittle Crack Propagation and Arrest in Japan," in Fracture Mechanics Technology Applied to Material Evaluation and Structure Design, edited by G.C. Sih, N.E. Ryan, and R. Jones, published by Martinus Nijhoff, The Hague, (1983).

6.) Instrumentation in Scientific Research Electrical Input Transducers, by K.S. Lion, McGraw-Hill, New York, (1959).

7.) Data-Acquisition Databook 1984, Volume 1, Integrated Circuits, Published by Analog Devices, Inc., 1984.